[7] F. W. Young, Jr., J. W. Cathcart, and A. T. Gwathmey, Acta Met. **4,** 145 (1956).
[8] T. B. Grimley and B. M. W. Trapnell, Proc. Roy. Soc. (London) **A234,** 405 (1956).
[9] W. E. Garner, F. S. Stone, and P. F. Tiley, Proc. Roy. Soc. (London) **A211,** 472 (1952).
[10] J. Bardeen, Phys. Rev. **71,** 717 (1947).
[11] A. Many, Y. Goldstein, and N. B. Grover, *Semiconductor Surfaces* (North-Holland, Amsterdam, 1965), pp. 131–136.
[12] Kelvin, Phil. Mag. **46,** 91 (1898).
[13] W. A. Zisman, Rev. Sci. Instr. **3,** 367 (1932).
[14] W. M. H. Sachtler, G. H. H. Dorgelo, and A. A. Holscher, Surface Sci. **5,** 221 (1966).
[15] T. B. Grimley, in *Chemistry of the Solid State,* edited by W. E. Garner (Butterworths, London, 1955), p. 360.
[16] W. E. Campbell and U. B. Thomas, Trans. Electrochem. Soc. **91,** 345 (1947).
[17] C. Wagner and H. Hammen, Z. Physik. Chem. **B40,** 197 (1938).
[18] K. R. Lawless and A. T. Gwathmey, Acta Met. **4,** 153 (1956).

THE JOURNAL OF CHEMICAL PHYSICS VOLUME 57, NUMBER 11 1 DECEMBER 1972

Total Cross Sections for Formation of Ions from CsBr by Collision with Ar, Xe, and NaBr(Ar)*

L. G. PIPER,† L. HELLEMANS,‡ J. SLOAN,§ AND J. ROSS
Department of Chemistry, Massachusetts Institute of Technology, Cambridge, Massachusetts 02139

(Received 3 July 1972)

Measurements have been made by cross beam techniques on the absolute total cross section Q for formation of ions from CsBr in collisions with Ar and Xe, and relative total cross section for NaBr with Ar, in a range of relative kinetic energies (Xe: 12–120 eV; Ar: 20–125 eV). The absolute cross sections obtained for CsBr, with estimates of accuracy, are 5.0 ± 1.2 Å^2 for Ar and 12.6 ± 2.7 Å^2 for Xe at a relative kinetic energy of 46 eV. The energy dependence of the cross sections follows closely that predicted by the simple reaction model of hard spheres. A fit of this model to the measurements leads to estimates of threshold energies. Measurements have also been made on a crude energy analysis of the ions formed. About half the ions of either sign have laboratory energies below 5 eV and the remainder is distributed continuously over larger energies up to the maximum. Negative ions have somewhat lower energies than positive ones. The results are consistent with a knockout model of collisional dissociation to ions, with a preference for dissociation by collision of the rare gas atom with the heavy (positive) end of the molecule.

I. INTRODUCTION

The subject of collisional dissociation of metal halide molecules has been studied recently experimentally[1–6] and theoretically.[7–8] In this article we present measurements of the absolute total cross section as a function of energy for formation of ions from CsBr in collisions with Ar or Xe, the relative total cross section as a function of energy for formation of ions from NaBr with Ar, and a crude measurement of the energy of the ions produced in the CsBr–Xe case. The measurements are made with a crossed molecular beam technique and extend over a range of relative energies (Xe: 12–120 eV, Ar: 20–125 eV) not investigated previously. The purpose of this research is to (1) obtain information on the energy dependence of a reaction cross section over a large range of energy, (2) study the dynamics of dissociation reactions, and (3) contribute to the study of Born–Oppenheimer conditions in dissociation reactions.[4]

II. APPARATUS

A schematic diagram of the apparatus[9] is shown in Fig. 1. Two modular units are joined to form the vacuum shell; the units are forged aluminum cubes and were designed by W. R. Gentry. The side of each cube is 1 ft long and 8-in. holes are bored through each face. All components are mounted on flanges, which cover the cube faces. Each chamber is evacuated by a liquid N_2 baffled 6-in. oil diffusion pump to a base pressure of 10^{-7} torr. The alkali halide beam effusing from the oven is crossed in the scattering chamber with the fast neutral beam, which is produced in the source chamber.

A plasma source similar to one described by Menzinger and Wahlin[10] generates the noble gas ions. By substituting 0.38 mm diameter tantalum wire for the tungsten which they used, longer filament lifetimes and less contamination of the insulating parts in the source result, due in part to the lower sputtering coefficient of tantalum.[11] The arc current is regulated to better than 0.1% by controlling the temperature of the filament with negative feedback, derived from the arc circuit and imposed on the filament power supply (operational amplifier type). The voltage drop in the source[12] $V_{1,2}$, see Fig. 1, is kept lower than the sum of the first and second ionization potential of the gas ($V_{1,2}$ is typically 37 V for Ar, 27 V for Xe). The source pressure is calculated to be in the range of 5 to 10×10^{-3} torr, in which case the source chamber pressure rises to about 7×10^{-7} torr.

Ions are extracted from the source through a 0.34 mm diameter hole (0.25 mm for the Xe runs) in the anode (2) and focused by a cylindrical decelerating saddle-field lens (3–5). Lens 5 is always at ground potential.

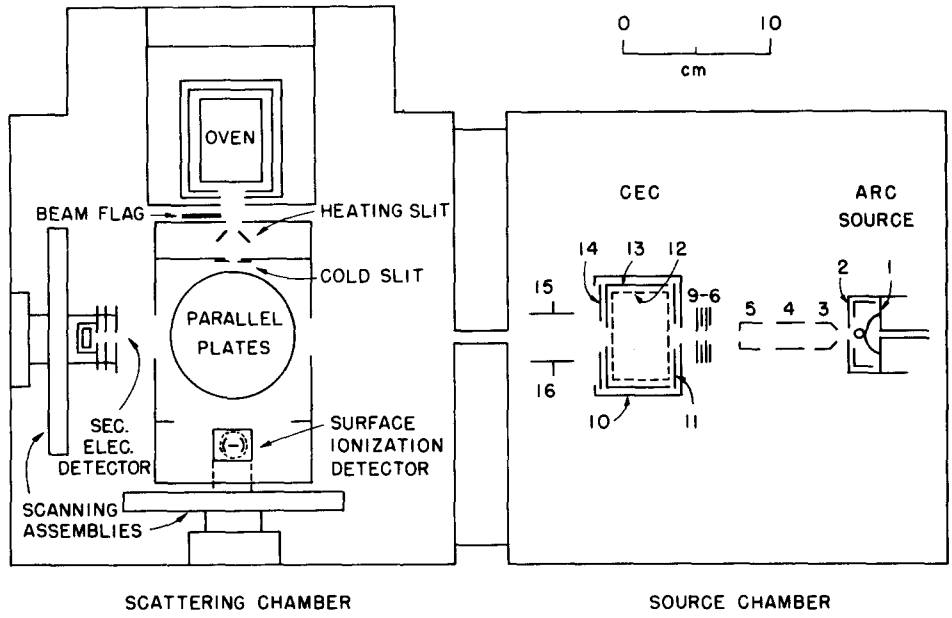

FIG. 1. Top view of the apparatus. Components are drawn to scale, except the arc source and the charge exchange chamber (CEC) which are stretched out vertically.

The focusing of the extracted ion beam is found to depend critically on the filament–anode distance and is also strongly related to the extraction field. Best focusing is obtained with a filament–anode distance of 4 mm and with 6–7 mm between anode and extractor lens (3). The ion–lens units are aligned axially to about 0.2 mm which is adequate.

In the absence of charge exchange gas, only the ions which flow through the charge exchange chamber (CEC) are potentially available for the formation of the fast neutral beam. The current of these ions may be measured by collecting them on plate 16 with the help of the repeller voltage $V_{15,16}$; this current is denoted by i_1^0.[13] Additional focusing is achieved by using aperture lenses 6–9 and entrance lens 10 as either one or two einzel lens units. A slight accelerating potential on lens 6 improves the focusing of low energy beams.

The ion beam is partially neutralized by symmetric charge exchange in the CEC, which is similar in design and operation to that described by Utterback and Miller.[14] The entrance (10) and exit (13) apertures of the cylindrical chamber have a diameter of 0.33 cm and are 5.20 cm apart. A measure of the focusing quality of the apparatus can be obtained from the ratio i_2^0/i_1^0, where i_2^0 is the intensity of diverging ions on the cup (13). Typical values are given in Table I. The pressure in the CEC, calculated on the basis of reported charge transfer cross sections for Ar[15] and Xe,[16] is about 1×10^{-3} torr. The source chamber pressure under those conditions rises to about 10^{-5} torr. Both elements 11 and 13 are kept at 5 V positive, in order to differentiate between scattered fast ions and slow ions resulting from charge exchange. The slow ion current i_3 is collected on grid 12, which is grounded through the picoammeter, whereas fast ions will easily overcome the small repulsive potential of the cup (elements 11 and 13).

The nominal ion energy is defined by the potential difference between anode 2 and the charge exchange region (inside grid 12), which is always grounded. The CEC can act as a Faraday cup when a high voltage (200 V) on electrode 14 closes it electrically. It is used in this mode to measure the ion beam energy.

The geometry of the neutral beam is found by measuring the ejected electron current from a beryllium copper surface, upon which the beam impinges after passing through an aperture of 0.8 mm diameter in the surrounding shield. During operation this shield is maintained at 100 V positive with respect to the Be–Cu surface to insure complete removal of the ejected electrons. The assembly is movable in a plane perpendicular to the beam. Measurements of the emission coefficient as a function of the impact energy are available for Ar.[17] This method of detection is restricted at lower energies (about 60 eV for Ar, 100 eV for Xe) by a rapidly decreasing electron ejection coefficient, which is also roughly proportional to the inverse of the ion mass.[18]

The alkali halide beam effuses from a stainless steel single chamber oven. The oven block and front are heated independently by insulated tantalum resistors. Working temperatures range from 900 to 1000°K. Different exit holes were used: a 0.13 mm diameter thin-walled aperture (front A) and three different multichannel arrays, all consisting of stainless steel tubes 1.27 cm long: Front B has 64 channels of 0.13 mm inner diameter grouped in a square of 2.2 mm side. The arrays of both front C and D are constructed with 0.10 mm inner diameter tubes, 38 arranged in a double row of 4.1 mm height for C and 36 in a single

TABLE I. Typical rare gas beam characteristics.

	Ar			Xe		
E_{lab} (eV)	100	60	25	120	55	20
Arc current (mA)	70	70	40	90	70	40
$V_{1,2}$[a]	37	37	39	24	26	29
V_3	−75	−50	−20	−87	−90	−80
V_4	71	48	17	90	40	15
$V_{15,16}$	100	100	50	100	100	30
i_1^0 [b]	8.80	5.80	1.50	7.10	3.20	0.42
i_2^0/i_1^0	0.022	0.226	1.61	0.014	0.65	2.48
i_3^0	0.01	0.03	0.20	0.024	0.027	0.18
P (10^{-6} torr)[c]	6.8	8.5	9.5	8.8	11	10
i_1	4.20	2.14	0.42	2.55	0.64	0.090
i_2	1.11	1.42	1.05	0.90	1.13	0.36
i_3	3.00	3.00	2.30	3.10	3.00	1.00
i_N[d]	2.70	2.06	0.72	2.62	1.22	0.20

[a] All potentials in volts.
[b] All currents i in units of 10^{-8} A.
[c] Pressure in the source chamber, when neutralizing gas is admitted.
[d] This value includes corrections.

row of 7.8 mm height for D. Front types C and D extend the homogeneity of the beam in the vertical direction.

The alkali halide beam passes through cold shields, where scattered molecules are trapped. Further collimation is provided by two rectangular slits, the first consisting of nichrome ribbons heated to 800°K, the second cooled to liquid nitrogen temperature, and both typically 1.5 mm wide.

The alkali halide beam is monitored by surface ionization detection on rhenium.[19] The exposed area of the filament is 0.76 mm wide and 3.2 mm high. The detector scans the beam intensity in both horizontal and vertical directions.

Product ions formed are collected on a pair of 7.6 cm diameter circular plates suspended above and below the scattering volume. The lower plate is operated as a repeller to drive ions of either sign quantitatively to the collector plate which is grounded through the electrometer. A circular grid is inserted close to the plate at lower potential and biased at least 12 V more negative to suppress secondary electron emission from that plate.

The detector system is surrounded by a liquid nitrogen cooled copper box, which provides electrical shielding and some pumping on background gases. The pressure in the scattering chamber is about 2×10^{-7} torr under working conditions.

III. EXPERIMENTAL METHOD

The total cross section Q for formation of ions relates the current I of ions of a given sign flowing out of the collision volume τ to the reactant number densities N_1 and N_2 and the relative velocity v,

$$I=QN_1N_2v\tau. \quad (1)$$

In this section we discuss the determination of the experimental quantities necessary for a calculation of the cross section.

A. Energies of Beams

In these experiments the relative velocity is very nearly equal to the velocity of the fast atoms, even at the lowest energies used (for 20 eV Xe the laboratory velocity is more than 99.8% of v). The alkali halide molecules can therefore be considered to be stationary.

It is assumed that the fast neutrals formed by charge transfer have the energy distribution of the parent fast ions. Retarding field analysis of typical ion beams is shown in Fig. 2; the ion energy equals the nominal value $eV_{2,10}$ to within ±0.5 eV. The energy spread at half maximum is about 1.3 eV and independent of the beam energy. This value must be regarded as an upper limit to the real spread as a consequence of the intrinsic limitations of the method of analysis.[20] An unexplained peak of 5%–10% of the total intensity appears at 1.5 eV below the nominal energy. Any loss of energy by elastic scattering of the neutrals on background gas within the angle allowed by the apparatus geometry is negligible.

B. Intensity of Rare Gas Beam

Ideally, the fast beam has to traverse a homogeneous beam of constant width, so that the collision volume is well defined by the cross sectional area S of the fast beam and its path length λ through the crossed beam.

In this section we discuss how the necessary experimental quantities are obtained to calculate the total cross section from Eq. (1). The product N_1vS is the fast neutral beam intensity I_N, so that Eq. (1) can be rewritten

$$Q=I/(N_2\lambda I_N). \tag{2}$$

The neutral beam current is determined indirectly from CEC intensity measurements. The fraction of incoming ions which charge exchange is represented by $\beta=i_3/(i_1+i_2+i_3)$ and has typical values of 0.46 and 0.58, respectively, for the Ar and Xe experiments. Representative values for these currents are given in Table I. The probability of multiple collisions in the CEC is not negligible at the pressures used, for instance a neutralizing event can be followed by elastic scattering. We follow in part the derivation in Ref. 14. The net current of particles, including ions and neutrals scattered out of the useful beam direction, is defined as i_s. The intensity of the well focused neutral beam, I_N, will be the fraction of i_1^0 which charge exchanges and which does not scatter beyond a given angle:

$$I_N=\beta(1-i_s/i_1^0)i_1^0. \tag{3}$$

The ion current flowing out of the CEC will be given by the fraction of i_1^0 which neither charge exchanges nor scatters

$$i_1=(1-\beta)(1-i_s/i_1^0)i_1^0. \tag{4}$$

With Eqs. (3) and (4) the neutral beam intensity is given in terms of experimental quantities as

$$I_N=\beta i_1/(1-\beta)=i_3(1+i_2/i_1)^{-1}. \tag{5}$$

This equation takes into account only neutrals that indeed flow out of the CEC, even when the ratio i_2^0/i_1^0, the focusing quality, is unfavorable. However, this calculation does not allow for neutrals formed along the ion path outside the neutralization chamber. At the working pressures approximately 10% of the total ion current ($\sum i^0$) is lost either by charge exchange or by elastic scattering outside the CEC. The most substantial loss occurs at the entrance apertures 10, 11. If the fraction of current lost is $\gamma=(\sum i^0-\sum i)/\sum i^0$, then the calculated current I_N, Eq. (5), needs to be increased by the fraction of γi_1^0 which charge exchanges ($\alpha\gamma i_1^0$) without being scattered on the way through the CEC. The correction for neutrals formed along the ion path outside the neutralization chamber is

$$\alpha\gamma i_1^0\{1-[i_s/(1-\gamma)i_1^0]\}.$$

Hence the corrected expression for I_N is

$$I_N=\beta(1-\gamma)i_1^0\{1-[i_s/(1-\gamma)i_1^0]\}+\alpha\gamma i_1^0\{1-[i_s/(1-\gamma)i_1^0]\},$$

which, to first order in γ, becomes

$$I_N=\beta(1-\gamma)i_1^0\{1-[i_s/(1-\gamma)i_1^0]\}(1+\alpha\gamma/\beta)$$
$$=[i_3/(1+i_2/i_1)](1+\alpha\gamma/\beta). \tag{6}$$

We have assumed here the same cross section for neutral and ion scattering. CEC current measurements provide values for α, since it is understood as the ratio of the cross section of charge exchange to that of total attenuation for the given apparatus geometry. Over the energy range covered, α is found to be 0.6 for Ar and 0.7 for Xe. The average values for γ/β are 0.22 and 0.18, respectively. For both gases the correction to I_N results in a factor $(1+\alpha\gamma/\beta)$ equal to 1.13. An additional correction is made to I_N, arbitrarily used whenever the background current i_3^0 exceeds 5% of i_3. The approximate value of β is then calculated, so that $i_3^0(1-\beta)$ can be subtracted from i_3 for further computation.

It is found in measurements of i_3 as a function of the potential on elements 11 and 13 that the slow ions produced in the charge exchange process have higher than thermal energies. This is thought to be related in large part to the space charge of the fast ion beam, which establishes a repulsive potential proportional to the charge density per unit length or $I(M/\text{eV})^{1/2}$, with I being the current of the ions of mass M and energy eV.[21] In both the Ar and Xe experiments the ratio $(i_1^0+i_2^0)/V^{1/2}$ is found to be about $8\times10^{-9}A/V^{1/2}$ at all beam energies, and a linear dependence of the slow ion energy on $M^{1/2}$ is observed: $(M_{Ar}/M_{Xe})^{1/2}=0.55$ is to be compared with 1.5 eV/2.7 eV=0.56.

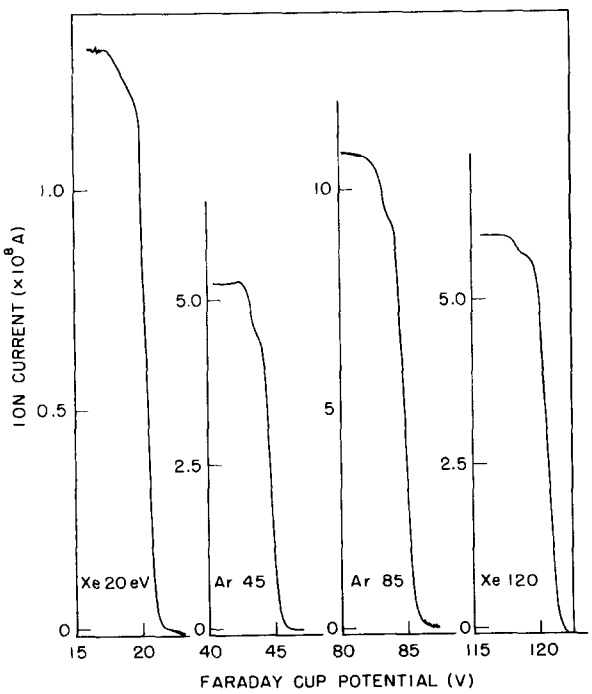

FIG. 2. Retarding field analysis of typical ion beams. For these measurements units 11, 12, 13 (Fig. 1) are shorted together to form a cup, and the potential is varied with respect to ground.

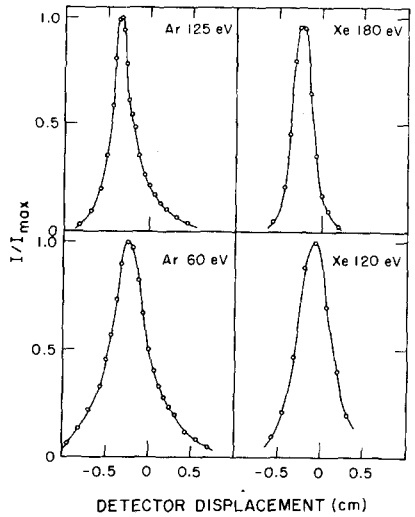

FIG. 3. Vertical profiles of rare gas beams (relative secondary electron current vs detector displacement). The origin indicates the geometrical center of the chamber. The range of the abscissa (~2 cm) corresponds to 3° angular spread.

C. Shape of Rare Gas Beam

Vertical and horizontal scans taken with the secondary electron detector show the beam to be almost cylindrically symmetric. Typical vertical profiles are presented in Fig. 3.

Aberrations of the focusing system are reflected in small deviations of the peak intensities from the geometrical center (up to 2.5 mm at the crossing point). The width of the profiles is variable with energy and focusing conditions. The maximum angular spread allowed by the apparatus geometry is 3°, when taking the middle of the CEC as origin. Observed profiles lie well within this limit.

With the use of efficiency factors for secondary emission,[17] the differential curves can be integrated to provide intensities of the Ar beam. The agreement with the calculations based on Eq. (6) is rather poor: the integrated current is an order of magnitude too small at 150 eV, but comes to within 30% of the calculated current at 60 eV. It is possible that the emission coefficient is not constant with beam density.[18]

D. Alkali Halide Beam

Characteristics of the alkali halide cross beam are found with the scanning surface ionization detector by measuring the beam current I_{MX} which strikes its surface A. The shape of the horizontal profiles is strongly dependent upon the beam intensity, showing progressively more broadening with increasing intensity as a consequence of scattering within the beam in the region between oven nozzle and cold slit. Nevertheless, measurements indicate the average width to be constant over the vertical extent of the alkali halide beam, with values ranging from 0.8 to 1.5 cm at the detector.

The product of the particle density and the average beam width, both measured at the detector, is equal to the flux $\int I_{MX} dl/A$ divided by the average speed $\bar{c}$ of the MX molecules. In order to deduce the value of this quantity in the scattering volume, a factor F for horizontal divergence of the beam and inverse square density dependence remains to be specified, so that

$$\lambda N_2 = F \int I_{MX} dl / A\bar{c}. \quad (7)$$

The oven temperature defines $\bar{c}$. An additional complication arises when the vertical intensity distributions are found to be nonuniform over the possible extension of the fast beam, as shown in Fig. 4. In order to account for this imperfection, the value of $\int I_{MX} dl$ at the maximum vertical intensity is multiplied by a factor of 0.90 ± 0.10 for the Ar runs, and 0.98 ± 0.02 for the Xe runs. The factor is rationalized as a compromise between crossing with an infinitely narrow beam and crossing with a homogeneous beam of 3° angular width.

A quadratic decrease in flux with distance is assumed for front types A and B so that F becomes the ratio of the distances from oven nozzle to the detector and to the scattering volume, respectively, $(F=1.69)$. A different expression is used for F in experiments with front C or D. It is taken as the ratio of extent of constant vertical intensity at the detector to that in the collision volume, with the assumption that the cold slit acts as a uniform source over its whole length (typically 6.2 mm high and F is approximately 1.3).

The alkali halide density obtained in the collision volume is approximately 1×10^9 molecules cm^{-3}.

E. Product Ion Current

The last quantity to be determined in Eq. (2) is the product current I. Product ion currents measured

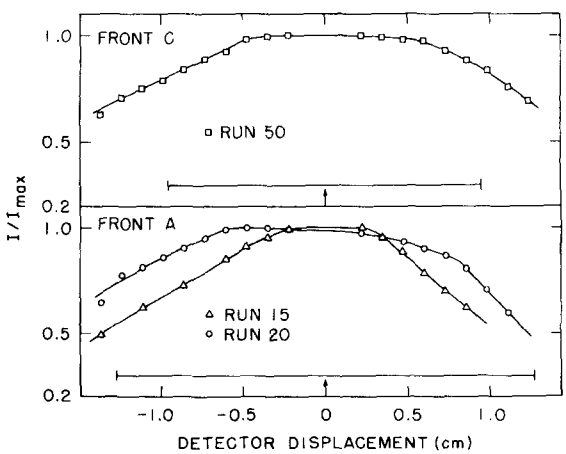

FIG. 4. Vertical profiles of the CsBr beam (relative surface ionization current I/I_{max} vs detector displacement) for two oven fronts (see Sec. II). The arrow indicates the geometrical center of the chamber. The profiles have been corrected for the detector height. The line segments indicate the extent of the rare gas beam with a 3° angular spread [scaled appropriately by the factor F, Eq. (7)].

range from 0.1 to 7×10^{-14} A with a noise level of about 5×10^{-16} A. Several processes contribute to the total current recorded on the parallel plate detector. The experimental procedure distinguishes the ions formed by collision of fast neutrals with alkali halide molecules from extraneous ion sources in the following way. When the alkali halide beam is shut off by a beam-flag, the detector signal includes electrons ejected from the walls by impinging fast atoms together with the products of ionization of background gas by the same particles. The signal measured when the beams cross will, after subtraction of the former signal, still contain the undesired contribution of ions leaking in from hot surfaces such as the oven, heated slit and surface ionization filament, combined with ions from the dissociation of alkali halide by high energy photons and thermal metastables emanating from the ion source. These effects are sorted out as the difference in signals with the alkali halide beam on and off and no neutralizing gas present in the CEC.

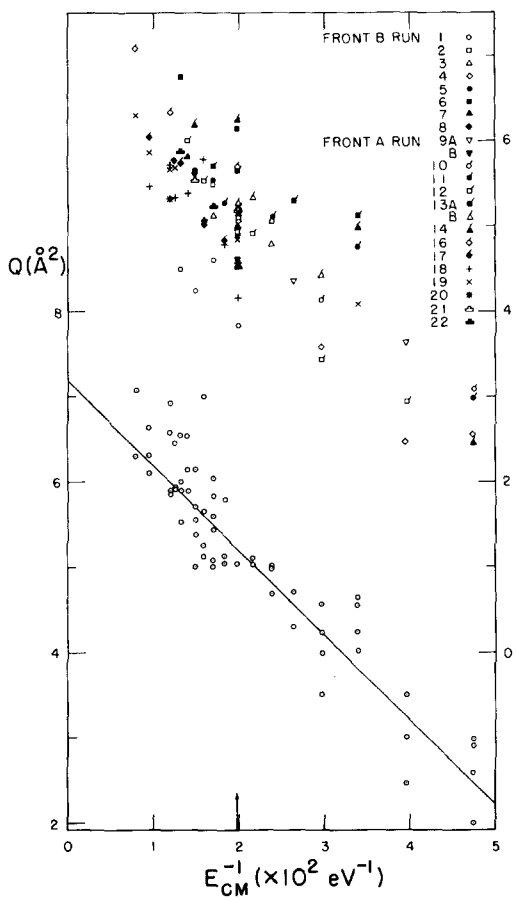

FIG. 5. Upper plot, ordinate on right: Absolute cross section (Å²) for ion formation, Ar+CsBr, vs reciprocal of initial relative kinetic energy, E_{CM}(eV). Front A and B refer to different exit orifices on the alkali halide beam source (see Sec. II). Lower plot, ordinate on left: Same as upper plot but points are normalized to the average cross section obtained at laboratory energy of 60 eV, $Q=5.04\pm0.30$ Å² (arrow). The line is a least square fit to the points.

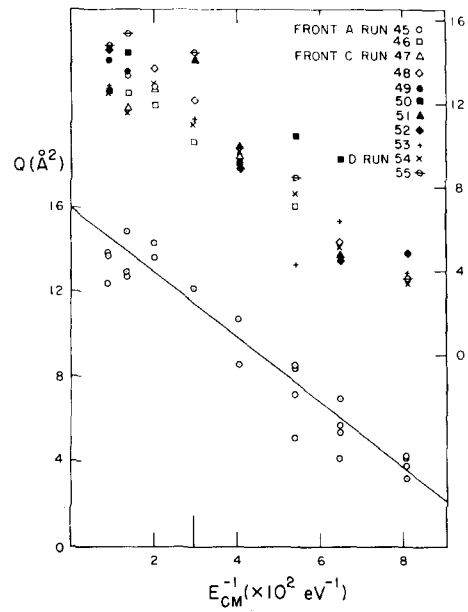

FIG. 6. Upper plot, ordinate on right: Absolute cross section (Å²) for ion formation, Xe+CsBr, vs reciprocal of initial kinetic energy, E_{CM}(eV). Front A, C, and D refer to different exit orifices on the alkali halide beam source (see Sec. II). Lower plot, ordinate on left: Same as upper plot but points, where possible, are normalized to the average cross section obtained at a laboratory energy of 55 eV, $Q=12.2\pm1.7$ Å² (arrow). The line is a least square fit to the points.

F. Composition of Rare Gas Beam

The fast ion beam possibly contains impurities other than neutrals and metastables at thermal energies. The choice of the voltage drop in the ion source $V_{1,2}$ precludes the formation of doubly charged species or high energy metastable ions[22] by single electron impact on atoms. They can be formed, however, by electron impact on a singly charged ion, as a phenomenon strongly localized in the cathode fall region. Extraction of these species through the anode is thus unlikely. Hagstrum reports the existence of low energy metastable ions for both Ar and Xe in an electron bombardment source.[23] Their concentrations are at most 1.5% of the ground-state ion abundance. There is uncertainty about their fate in the charge exchange region, but neutralization to metastables is improbable, be that only on the basis of the energy defect involved. Other alternatives such as

$$^{m}Y^{+}+Y\rightarrow Y^{+}+Y^{+}+e^{-}$$

will at worst slightly alter the calculation of I_N.

There is a possibility of molecular ions Y_2^+; their concentration is estimated to be less than one percent of the ground-state ion concentration at the pressures used in the ion source.[24] Neutrals eventually resulting from their neutralization in the CEC will have half of the nominal beam energy.

The neutralizing process itself will also add a small fraction of metastables to the fast beam. For Ar, some

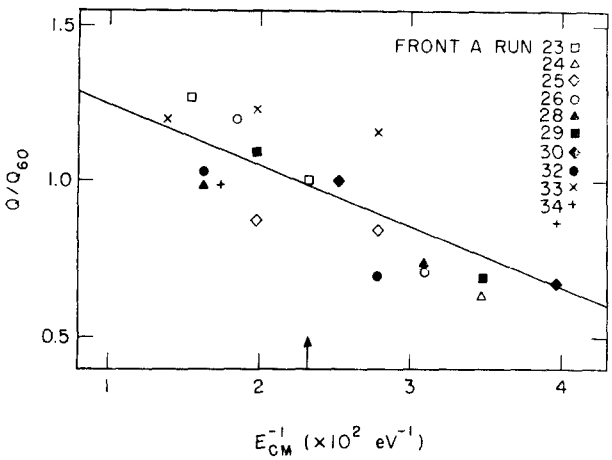

FIG. 7. Cross section for ion formation, Ar+NaBr, vs reciprocal of initial relative kinetic energy, E_{CM}(eV), normalized to an arbitrarily assigned value of 1 Å² at a laboratory energy of 60 eV (arrow). Front A refers to the type of exit orifice on the alkali halide beam source (see Sec. II). The line is a least square fit to the points.

0.003% of the ions which charge exchange are reported to yield metastables of about 11.5 eV.[25] Another 1% are neutralized on their way through the lenses. These atoms will have energies which depend on the potential of the neutralization region, and will broaden the energy spectrum of the fast beam, mostly on the low energy side.

Impurities in the rare gas beam will not have the drastic effects here as are expected for processes where the cross section sweeps through several orders of magnitude in the energy range studied.

IV. RESULTS AND DISCUSSION

A. Experimental Results and Estimate of Accuracy

The experimental cross sections for diabatic dissociation of CsBr by Ar and Xe are plotted in Figs. 5 and 6 as a function of the reciprocal of the center of mass (c.m.) energy. The upper series of points in each figure shows the reproducibility. The measurements of each run, taken on a certain day with the same experimental setup, have individual symbols.

To improve the internal consistency of the various runs, the measurements are also shown normalized to the average value of all determinations at a reference laboratory energy (the lower set of points in Fig. 5 and 6). For the Ar+CsBr system the reference is at a laboratory energy of 60 eV with $Q=5.04\pm0.30$ Å², a value obtained by averaging 23 runs at that energy. For the Xe+CsBr system the reference is chosen at 55 eV with $Q=12.2\pm1.7$ Å² (six runs). Only a limited number of runs contain a measurement at this energy and are thus fit for normalization. The reported values for Q are absolute cross sections and the standard deviation given reflects the precision of the measurements.

Results for the system Ar+NaBr are shown in Fig. 7 normalized to an arbitrary value of $Q=1$ Å² at 60 eV laboratory energy. No absolute values for the cross section of dissociation into ions are given here because of the uncertainties in the performance of the surface ionization detector and the unknown contribution of dimers to the formation of ions in collisions with fast atoms. With the (doubtful) assumption that dimers do not dissociate diabatically under atomic impact and the (generally accepted) assumption that surface ionization produces two positive ions for each dimer striking the rhenium filament, cross sections of the same magnitude as that for the Xe+CsBr system are obtained.

The surface ionization efficiency of oxygenated rhenium is reported to be 100% for CsBr and NaBr.[19] This condition will in theory last as long as the filament temperature is high but does not exceed 1750°K. In these experiments the operating temperature is in the 1500–1600°K range. However, a fast decrease of the metal's work function is observed in the NaBr experiments, and high intensities even of CsBr seem to contaminate the surface after several days of continuous use.

Miller and Kusch[26] find a negligible fraction of dimers (less than 1.5%) in an effusive molecular beam of any of the cesium salts. About 20% of the effusing particles are dimers for NaI and NaCl at oven pressures of 10^{-2} torr.

Measurements of a crude energy analysis on ions formed in the system Xe+CsBr at 120 eV laboratory energy are shown in Fig. 8 for several runs. The ion current, corrected for variations of I_{MX}, is measured as a function of the repeller plate voltage. In this case the grids are kept at the same potential as the plates, which they guard. An ion with laboratory energy E_{lab}, which is moving in the plane of the beams, will just be collected by a repeller voltage of 1.5 E_{lab}/e as a consequence of the geometrical arrangement.

We conclude the presentation of experimental results with an estimate of the random error for the absolute cross sections of diabatic dissociation of CsBr with Ar and Xe. The uncertainty of both the ion current collected on the parallel plates and of the measurements of $\int I_{MX} dl$ at the surface ionization detector is 3%. The neutral beam intensity is believed to be determined to within ±20%[14] and the oven temperature is known to about ±5%. The average correction for the imperfect crossing of the beams can be in error by ±10% for the Ar and ±2% for the Xe runs and finally the correction F for divergence of the alkali halide beam is uncertain by ±8%. When these errors are combined, a random error of 24% is found for the Ar+CsBr and 22% for the Xe+CsBr experiments. Hence, the absolute cross sections for diabatic dissociation of CsBr on impact with Ar, Xe as deduced from this work are: $Q=5.0\pm1.2$ Å² for Ar and $Q=12.6\pm2.7$ Å² for Xe at a relative kinetic energy of 46 eV. The data have been

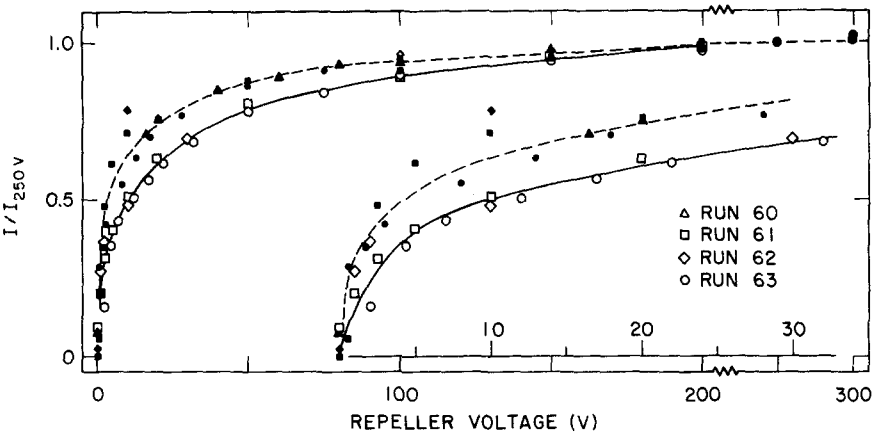

FIG. 8. Product ion current I as a function of the repeller plate voltage for Xe+CsBr, laboratory energy 120 eV. Currents are given relative to the value recorded at ±250 V on the repeller. Positive ion current —, negative ion current - - -. The inset shows detail of the low energy region.

collected at various oven temperatures, implying a variable vibrational energy in the alkali halide. Near reaction threshold a sensitive dependency of the collision-induced dissociation on vibrational excitation has been established[5] and theoretically corroborated.[7] The effect is unimportant in our energy range.

Determinate errors may occur due to the contribution to the ion current of other than diabatic dissociation events. Table II shows possible ion-producing reaction channels for our systems. The presence of dimers extends still further the choice of possible reaction paths and mass selection of the products is necessary to distinguish between them. The striking effect of minute amounts of Tl_2Br_2 on the value of the total cross section for production of positive ions resulting from collisions with accelerated atoms has been shown by Parks and Wexler.[6] We shall consider the CsBr beam to be free of dimerized species.

Reaction (1) in Table II is the object of this study. Composite ionization processes comparable to Reactions (2)–(4) in Table II have cross sections that rise steeply with c.m. energy from approximately 0.005–0.05 Å^2 at 20 eV above threshold to 0.1–1.0 Å^2 at 100 eV above threshold.[27] Their contribution to Reaction (1) is therefore small. A rearrangement reaction such as (5), Table II, is observed in the dissociation of TlBr by Xe,[6] but not in the dissociation by Kr. The cross section for this process is roughly 0.03 Å^2 at 8.5 eV c.m. energy and has decreasing relative importance to the total positive ion current as the relative kinetic energy increases.[28,6]

TABLE II. Energetics of reactions producing ions in atom–alkali halide collisions.

Process	Threshold energy (eV) CsBr	NaBr
(1) $A+MX \rightarrow A+M^+ + X^-$	4.72[a]	5.54[a]
(2) $A+MX^+ + e^-$	7.72[b]	~8.5[c]
(3) $A+M^+ + X + e^-$	8.08[a]	8.90[a]
(4) $A^+ + e^- + MX$	(Ar) 15.8[a]	15.8[a]
(5) $MA^+ + X^-$		

[a] L. Brewer and E. Brackett, Chem. Rev. **61**, 425 (1961); C. E. Moore, Natl. Bur. Std. (U.S.) Circ. **467** (1949); R. S. Berry and C. W. Reimann, J. Chem. Phys. **38**, 1540 (1963).

[b] J. Berkowitz, J. Chem. Phys. **50**, 3503 (1969).

[c] J. Berkowitz and W. A. Chupka, J. Chem. Phys. **29**, 653 (1958).

B. Discussion

Over the c.m. energy range from 10 to 100 eV above the threshold for diabatic dissociation the experimental cross sections can be well fitted to the energy dependency of a hard-sphere model: $Q = \pi d^2(1-D/E_{CM})$. D is the threshold of the dissociation process and d is the sum of the hard sphere radii of the colliding particles; the frequently appended steric factor has been set equal to unity. A least-squares fit to the normalized experimental values is drawn in Figs. 5–7. The intercepts can be translated into values for d and D, respectively, 1.51 Å and 13.9 eV for Ar+CsBr, 2.25 Å, and 9.6 eV for Xe+CsBr, and for Ar+NaBr, 13.5 eV. Qualitatively, it is reasonable to suppose that reaction probabilities extend to larger impact parameters for the Xe+CsBr pair, since ion-induced dipole polarization forces are larger than for Ar+CsBr. We emphasize that the numbers obtained for d and D, discussed further below, are derived from the hard sphere model in the stated energy range (10–100 eV). The measured threshold energies, determined with comparable kinetic energies (~5 eV), are the endoergicities.[5]

The threshold energies for this model (the parameter D) can be calculated from the high energy limit of the classical VT energy transfer problem.[29] In this model, dissociation occurs when the vibrational energy transferred equals the bond energy of the oscillator. For the calculations this energy is taken as the endoergicity of the diabatic dissociation. The theoretical values are then 14.9 and 7.7 eV, respectively when

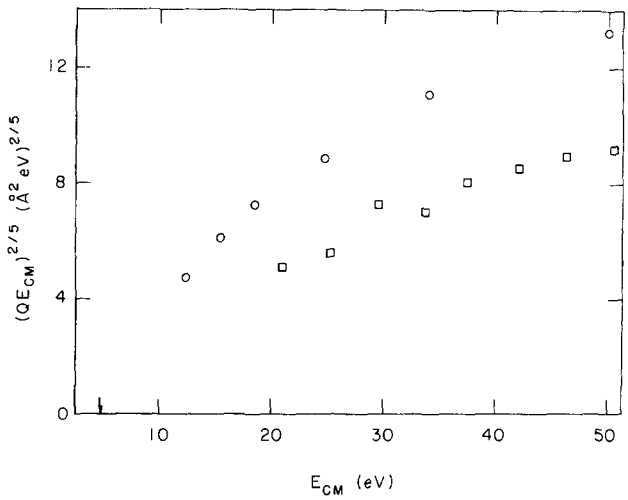

FIG. 9. Absolute cross section for ion formation Q times initial relative kinetic energy E_{CM}, to the two-fifth power vs E_{CM}. Circles: Xe+CsBr; squares: Ar+CsBr. The arrow indicates the threshold energy for diabatic dissociation of CsBr.

Ar and Xe hits the Cs end of the molecule. (With a refined approximation,[29] these values increase by about 9% and 14%). When the Br-end is struck, the thresholds are 7.2 and 4.9 eV. These two sets are to be compared with the experimental values of 13.9 and 9.6 eV. Apparently the best agreement is obtained by considering effective dissociation to result from heavy-end collisions. For the Ar+NaBr system the theoretical values are 20.4 and 5.6 eV, respectively, for collisions on the Br and the Na end, to be compared with the experimental 13.5 eV. Again better agreement is recorded with the calculation for collision on the heavier end. This conclusion obtained from measurements at high energies differs from that of the exact classical calculations of Kelley and Wolfsberg[30] on energy transfer at lower kinetic energies in a model of an atom interacting by repulsive forces with a harmonic oscillator or Morse oscillator, and the experimental results of Tully, Lee, and Berry,[5] also at lower kinetic energies, where it is shown that translational energy is transferred most efficiently to internal degrees of freedom in collisions of the atom with the light end of the diatomic molecule. A recent calculation, however, on a one-dimensional model,[8b] shows the Cs–Xe collision to be more effective than the Xe–Br collision, when use is made of a "soft" interaction potential between the atom and alkali halide.

The differences observed in the two systems Ar+CsBr, Xe+CsBr, and those deduced from a hard-sphere model, lead to the conclusion that diabatic dissociation at higher energies likely does not occur on collision by excitation of CsBr to a dissociative electronic state and subsequent dissociation to ions. If that mechanism were operative, the threshold energies would be independent of the rare gas atom.

An optical model analysis has been made for the energy dependence of the cross section near threshold for collision-induced dissociation to a three-body final state.[8] In the post-threshold region the cross section is of the form $Q\sim(E_{CM}-D)^{5/2}/E_{CM}$ provided the internal energy of the diatomic molecule is neglected. E_{CM} is the c.m. energy and D the threshold energy, in this case taken to be the dissociation energy to ions. In Fig. 9 values of $(QE_{CM})^{2/5}$ are plotted against E_{CM} for both the Ar–CsBr and Xe–CsBr systems. No linear relation is obtained in the energy range studied, as expected from the comparison with the hard sphere model, but in the low energy limit the predicted behavior seems likely. (In the Ar+CsBr system there may be a trend of the experimental cross sections away from the hard-sphere model (straight line, Fig. 5) at c.m. energies above 74 eV.)

The integrated distribution curves in Fig. 8 are smooth for both the positive and negative ions, indicating that no particular reaction channel is favored at this high impact energy. The negative ions have less energy, and about 13% of their total is steadily collected over and above the positive ion current at the lower repeller voltages. The energy distributions for the ions approach zero at about 200 V on the repeller. The ion products at these large energies can be identified with the relatively rare impulsive head-on collisions, which are accompanied by a nearly complete energy transfer. About half of the ions of either sign have very low laboratory energy (<5 eV) while the remainder is distributed continuously over the range of laboratory energies up to the maximum. These results can be understood qualitatively by assuming that the diabatic dissociation proceeds in the present range of relative energy by a knockout mechanism. In this model it is assumed that the impinging atom hits the CsBr on either end. In the process of loosening the bond, no momentum is transferred to the ion not hit directly by the rare gas atom, and this ion will, after dissociation, appear as a slowly drifting ion in laboratory coordinates. The collision-induced dissociation of ion–molecules at high relative energies has been explained successfully by this mechanism.[31] It was found by differential energy analysis that the peak of the velocity distributions of the forward scattered fragment ions coincided with the velocity of the accelerated parent diatomic ion–molecules. The total cross sections in that case were found to be about an order of magnitude smaller than in the present study.

The negative current at low ion energy is larger than the positive one (Fig. 8) and this may indicate again a higher efficiency for dissociation when the heavy end (Cs) of the molecule is struck: the role of the spectator in the knockout mechanism is assumed more often by Br than by Cs. However dissociation processes with electrons as one of the products yield low energy ($\sim$0 eV) negative species and a broad spectrum of positive ions.[32] A quantitative account of the difference between the positive and negative current would require

a correction due to the possible production of electrons in collisions. In addition, in an impulsive collision the energy transfer may approach 100% for Xe–Cs but only 94% for Xe–Br; this mass effect tends to produce Br^- ions with lower speeds than Cs^+ ions.

The cross sections obtained in this study are smaller than the minimum of 10 Å², at 1 eV above threshold, reported for the Xe+CsBr system.[5] Furthermore in the present energy range we do not find a large difference between the cross sections for Xe+CsBr and Ar+CsBr, as the order of magnitude difference in the reactions Xe+TlBr and Kr+TlBr.[6]

ACKNOWLEDGMENT

We thank John Winn for his help in some of the construction of the apparatus.

* Supported in part by the National Science Foundation and Project Squid of the U.S. Office of Naval Research.

† Present address: Department of Chemistry, Kansas State University, Manhattan, Kansas.

‡ In part "Aangesteld Navorser van het Belgisch Nationaal Fonds voor Wetenschappelijk Onderzoek."

§ Present address: Department of Chemistry, Queens University, Kingston, Ontario.

[1] R. S. Berry, T. Cernoch, M. Coplan, and J. J. Ewing, J. Chem. Phys. **49,** 127 (1968).

[2] R. Hartig, H. A. Olschewski, J. Troe, and H. G. Wagner, Ber. Bunsenges, Physik. Chem. **72,** 1016 (1968).

[3] A. Mandl, E. W. Evans, and B. Kivel, Chem. Phys. Letters **5,** 307 (1970); A. Mandl, J. Chem. Phys. **55,** 2918 , 2922 (1971).

[4] J. J. Ewing, R. Milstein, and R. S. Berry, J. Chem. Phys. **54,** 1752 (1971).

[5] F. P. Tully, Y. T. Lee, and R. S. Berry, Chem. Phys. Letters **9,** 80 (1971).

[6] E. K. Parks and S. Wexler, Chem. Phys. Letters **10,** 245 (1971).

[7] R. D. Levine, Chem. Phys. Letters **11,** 109 (1971).

[8] (a) R. D. Levine and R. B. Bernstein, Chem. Phys. Letters, **11,** 552 (1971). (b) H. Fan, J. Chem. Phys. **55,** 4628 (1971).

[9] L. G. Piper, "Dissociation of Alkali Halides in Collisions with High Energy Argon," Ph.D. thesis, M.I.T., Cambridge, Mass., 1971.

[10] M. Menzinger and L. Wåhlin, Rev. Sci. Instr. **40,** 102 (1969).

[11] J. D. Cobine, *Gaseous Conductors* (McGraw-Hill, New York, 1941), p. 230.

[12] A voltage with two numbers as subscript denotes the voltage between the components so numbered in Fig. 1. A voltage with one number as subscript denotes the potential of the component so numbered with respect to ground.

[13] The superscript ° denotes a current measured in the absence of neutralizing gas.

[14] N. G. Utterback and G. H. Miller, Rev. Sci. Instr. **32,** 1101 (1961).

[15] W. H. Cramer, J. Chem. Phys. **30,** 641 (1959).

[16] J. A. Dillon, Jr., W. F. Sheridan, H. D. Edwards and S. N. Ghosh, J. Chem. Phys. **23,** 776 (1955).

[17] P. O. Haugsjaa, J. F. McIlwain, and R. C. Amme, J. Chem. Phys. **48,** 527 (1968).

[18] R. C. Amme, J. Chem. Phys. **50,** 1891 (1969).

[19] A. Persky, J. Chem. Phys. **50,** 3835 (1969).

[20] J. A. Simpson, Rev. Sci. Instr. **32,** 1283 (1961).

[21] G. R. Brewer, in *Focusing of Charged Particles,* edited by A. Septier (Academic, New York, 1967), Vol. II, p. 76.

[22] J. Wm. McGowan and L. Kerwin, Can. J. Phys. **41,** 1535 (1963).

[23] H. D. Hagstrum, Phys. Rev. **104,** 309 (1956).

[24] J. P. Gaur and L. M. Chanin, Phys. Rev. **182,** 167 (1969).

[25] P. O. Haugsjaa, R. C. Amme, and N. G. Utterback, Phys. Rev. Letters **22,** 322 (1969).

[26] R. C. Miller and P. Kusch, J. Chem. Phys. **25,** 860 (1956).

[27] N. G. Utterback, *Advances in Applied Mechanics,* edited by L. Trilling and H. Wachman (Academic, New York, 1969), Suppl. 5, Vol. II, p. 1379.

[28] K. Lacmann and A. Henglein, Ber. Bunsenges. Physik. Chem. **69,** 286 (1965); T. F. George and R. J. Suplinskas, J. Chem. Phys. **51,** 3666 (1969).

[29] B. H. Mahan, J. Chem. Phys. **52,** 5221 (1970).

[30] J. D. Kelley and M. Wolfsberg, J. Chem. Phys. **53,** 2967 (1970).

[31] See J. Schöttler and J. P. Toennies, Chem. Phys. Letters **12,** 615 (1972), and references cited.

[32] R. H. Hammond, J. M. S. Henis, E. F. Greene, and J. Ross, J. Chem. Phys. **55,** 3506 (1971).